

Mathematical modelling of zika virus in Brazil

Saúl E. Buitrago Boret^{a,*}, René Escalante^a, Minaya Villasana^a

^a*Dpto. Cómputo Científico y Estadística, Universidad Simón Bolívar, Caracas, Venezuela*

Abstract

In this paper we study some deterministic mathematical models that seek to explain the expansion of zika virus, as a viral epidemic, using published data for Brazil. SIR type models are proposed and validated using the epidemic data found, considering several aspects in the spread of the disease. Finally, we confirmed that the crucial epidemic parameter such as R_0 is consistent with those previously reported in the literature for other areas. We also explored variations of the parameters within Brazil for different federal entities. We concluded that a parsimonious model that includes both human and vector populations best describe the epidemic parameters.

Keywords: Mathematical modelling, zika, SIR, epidemiological modelling

1. Introduction

The zika virus (ZIKV) was first isolated in 1947 from a sentinel rhesus monkey in the Zika forest in Uganda (see [9]) and was classified by sequence analysis into two genotypes, African and Asian (see [15]). In April 2007, a large epidemic of Asian genotype ZIKV was reported in Yap Island and Guam, Micronesia. Between 2013-2014 the Asian genotype caused epidemics reported in several Pacific Islands, including French Polynesia, New Caledonia, Cook Islands, Tahiti, and Easter Island. (see [14] and [1]).

In a general review published in 2014 by Ioos et al. [18] it was reported

*Corresponding author

Email addresses: sbutrago@usb.ve (Saúl E. Buitrago Boret), rescalante@usb.ve (René Escalante), mwillasa@usb.ve (Minaya Villasana)

that the ZIKV infection caused two major epidemics in Pacific previously naive territories, in less than a decade. This emergent arbovirolosis transmitted by mosquitoes of the *Aedes* genus has a high potential for spreading in countries where the vector is present.

In March 2015, the first endogenous transmission of Zika virus in Brazil was reported. Beginning 2015, many patients came to health services in the state of Rio Grande do Norte presenting dengue-like symptoms. However, physicians and initial laboratory tests ruled out the presence of both dengue virus and chikungunya. Some samples of these patients were transferred to the Instituto Oswaldo Cruz (world leader in research on tropical diseases) where they performed very sensitive screening DNA virus, the results were consistent with those expected for the presence of Zika. The issue becomes very serious and worrisome from May 2015, when the first case of a fetus with microcephaly whose mother had suffered a Zika infection was detected. It may have been a fluke, but cases of microcephaly have grown exponentially in the geographical areas where the Zika virus is present (see [16, 3, 28]). In fact, Zika intrauterine infection has been reported by detecting the virus in the amniotic fluid of some pregnant patients (see [24, 30, 8]). A recently published modelling study conducted in French Polynesia, where a documented outbreak of Zika virus infection occurred in 2013, retrospectively estimated the risk to be 95 cases of microcephaly per 10000 women infected during the first trimester (see [19]). Moreover, a rare complication of Zika virus infection can lead to neurological and autoimmune disorders such as Syndrome Guillain-Barre. In fact there are certain press releases that summarize the increase of this syndrome in patients who have overcome the disease (see [35]).

In the following months ZIKV was reported in several countries of South and Central America, and the Caribbean. Fig. 1 (Source: Washington Post; Credit: Laris Karklis) shows graphically the propagation of zika virus from 1947 to 2015.

Recent studies in mice suggest that the virus could attack the adult brain as well (see [2] and [25]).

ZIKV infection, together with dengue and chikungunya, are one of the leading

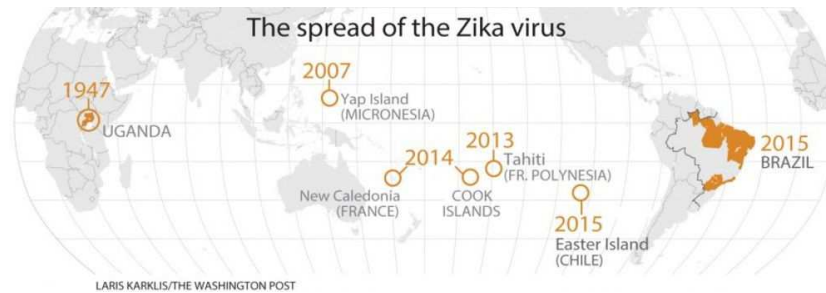


Figure 1: Propagation of zika virus from Zika forest in Uganda (1947) to Brazil (2015). Source: Washington Post; Credit: Laris Karklis.

causes of illness in the tropics and subtropics, where it inflicts substantial health, economic and social burdens. Humans are infected with zika virus by the bite of an infective female mosquito *Aedes aegypti*, the principal vector of zika. Once a person gets bitten by an infective mosquito, the virus undergoes an incubation period of about 3 to 12 days, after which the person enters the acute phase of infection. The acute phase can be as short as 2 days and as long as 7 days. If other female *Aedes aegypti* mosquitoes bites the ill person during this acute phase, those mosquitoes may become infected and subsequently begin the transmission cycle anew. Fig. 2 (Source: CDC, PLOS, Reuters; Credits: David Foster, Laurie Garrett, Doug Halsey and Gabriela Meltzer) shows graphically how zika virus enters the human population.

Many people infected with zika virus will not have symptoms or will only have mild symptoms. The most common symptoms of zika are fever, rash, joint pain, conjunctivitis (red eyes), muscle pain and headache. Zika is usually mild with symptoms lasting for several days to a week. People usually do not get sick enough to go to the hospital, and they very rarely die of zika. For this reason, many people might not realize they have been infected. Symptoms of zika are similar to other viruses spread through mosquito bites, like dengue and chikungunya.

There is scientific consensus that zika virus is a cause of microcephaly and Guillain-Barré syndrome (see [35]). Links to other neurological complications

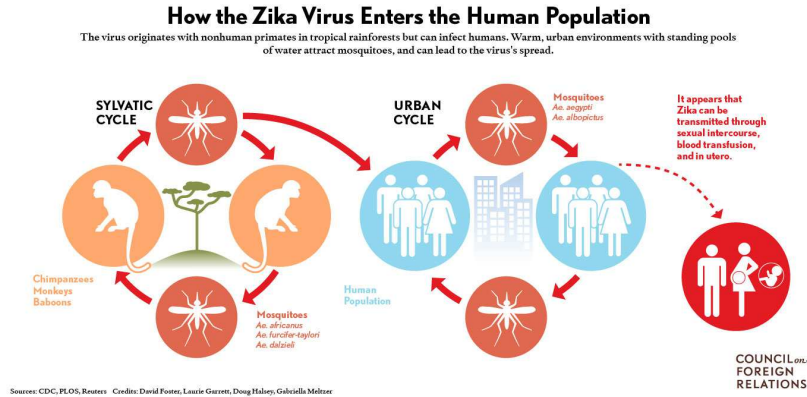


Figure 2: How the zika virus enters the human population. Source: CDC, PLOS, Reuters; Credits: David Foster, Laurie Garrett, Doug Halsey and Gabriela Meltzer.

are also being investigated. Sexual transmission of zika virus is also possible. Other modes of transmission such as blood transfusion are being investigated.

The foundations of the entire approach to epidemiology, based on compartmental models, were laid by public health physicians such as Sir R.A. Ross [29], W.H. Hamer, A.G. McKendrick, and W.O. Kermack [20, 21, 22] between 1900 and 1935, along with important contributions from a statistical perspective by J. Brownlee [6, 12].

Mathematical models have been extensively used to study the dynamics of infectious diseases at population level. Most continuous time models are in the form of ordinary differential equations (ODEs). Such ODE models assume that the population is well mixed, and the transmission is instantaneous (see [4, 5]).

Mathematical modelling is typically the only way to examine the possible impact of different release and control scenarios. Questions that can be addressed are, for instance, what fraction of the population should be quarantined and/or vaccinated? How fast can control measures to be implemented?, etc.

The basic reproductive ratio (see [10, 11] and [17]), R_0 , is defined as the expected number of secondary infections arising from a single individual during his or her entire infectious period, in a population of susceptibles. R_0 often

serves as a threshold parameter that predicts whether an infection will spread. Determining R_0 is vital to understand and characterize the dynamics of the disease. However this crucial parameter is model dependent. We study and calculate R_0 using different modelling perspectives that can allow us to draw better conclusions on its validity and range. Also, this parameter is investigated at different granularity levels: country wide and state wide.

This paper, based on the preliminary work by Buitrago *et al.* [7], is organized as follows: section 2 outlines the mathematical models used, section 3 briefly describe details around the basic reproductive ratio R_0 for the models developed in section 2, section 4 provides information about the data used and in the last section, section 5, a discussion of the methodologies and their application to the data sets are summerized.

2. Mathematical Modelling

We formulate our descriptions as compartmental models, with the population under study being divided into compartments and with assumptions about the nature and time rate of transfer from one compartment to another.

In formulating models in terms of the derivatives of the sizes of each compartment we are also assuming that the number of members in a compartment is a differentiable function of time. This assumption is plausible once a disease outbreak has become established but is not valid at the beginning of a disease outbreak when there are only a few infectives.

In this work we describe models for epidemics, acting on a sufficiently rapid time scale that demographic effects, such as births, natural deaths, maintain a constant level of the overoll population, and migration may be ignored.

All the models considered in this work satisfy the following assumptions:

- There is homogeneous mixing, which means that individuals of the population make contact at random and do not mix mostly in a smaller subgroup.
- The disease is novel, so no vaccination is available and or applied.

- Any recovered person has permanent immunity or least considered as such within the time-frame of the disease.
- The population size is constant for the models.

2.1. SIR model

Consider a population in which a small number of its members suffer from an infectious disease that can be transmitted to other members of the same population. The objective we are pursuing now is to determine what proportion of the total population will be infected and for how long, using a mathematical model that incorporates into their structure the transmission mechanisms that we consider important.

In order to model such an epidemic we divide the population being studied into three classes labeled S , I , and R .

Let $S(t)$ denote the number of individuals who are susceptible to the disease, which can acquire the infection through contacts with infectious, that is, who are not (yet) infected at time t . $I(t)$ denotes the number of infected individuals, assumed infectious and able to spread the disease by contact with susceptibles. $R(t)$ denotes the number of individuals who have been infected and then removed from the possibility of being infected again or of spreading infection (see Fig. 3).

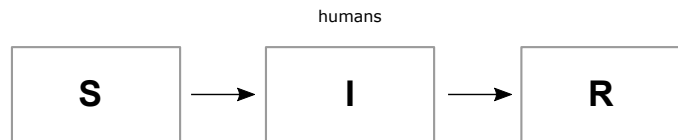


Figure 3: Structure of the SIR model.

Removal is carried out through isolation from the rest of the population, through immunization against infection, through recovery from the disease with full immunity against reinfection, or through death caused by the disease. These characterizations of removed members are different from an epidemiological per-

spective but are often equivalent from a modelling point of view that takes into account only the state of an individual with respect to the disease.

We will use the terminology SIR to describe a disease that confers immunity against reinfection, to indicate that the passage of individuals is from the susceptible class S to the infective class I to the removed class R . The mathematical model is:

$$\frac{dS}{dt}(t) = \mu N - \beta S(t)I(t)/N - \mu S(t), \quad (1)$$

$$\frac{dI}{dt}(t) = \beta S(t)I(t)/N - \gamma I(t) - \mu I(t), \quad (2)$$

$$\frac{dR}{dt}(t) = \gamma I(t) - \mu R(t), \quad (3)$$

$$\frac{dC_i}{dt} = p\beta S(t)I(t), \quad (4)$$

with the initial conditions in $t = t_0$

$$S(t_0) = S_0 > 0,$$

$$I(t_0) = I_0 > 0,$$

$$R(t_0) = R_0 > 0,$$

where S_0 , I_0 and R_0 are, respectively, the initial number of susceptible, infected and recovered people with β , γ and μ positive constants. As is often the case, not all infectives are symptomatic, specially in the Zika virus, and thus not all cases are reported as such making the determination of the real number of infectives a difficult task. In equation 4, C_i accounts for the cumulative infectives and is a smooth monotone function that is used for identification purposes. The parameter p is a proportion of the infectives that are reported. β is the transmission rate from mosquitoes to humans, γ is the per capita rate of recovery in humans such that $1/\gamma$ is the mean infectious period for humans, μ is the per capita rate of mortality in humans such that $1/\mu$ is the life expectancy of humans, and N is the human population size.

2.2. SIR/SI model

This model is an extension of the SIR model, and has been used before in the study of the dynamics of dengue in Thailand by Pandey *et al.* [27].

The population is divided into three classes for humans and two classes for mosquitoes or vectors that transmit the disease. S_H represents the number of susceptible, I_H the number of infectious, and R_H the number recovered individuals in the human sub-population. Similarly, S_v represents the proportion of mosquitoes currently susceptible, and I_v the proportion of infectious mosquitoes (see Fig. 4).

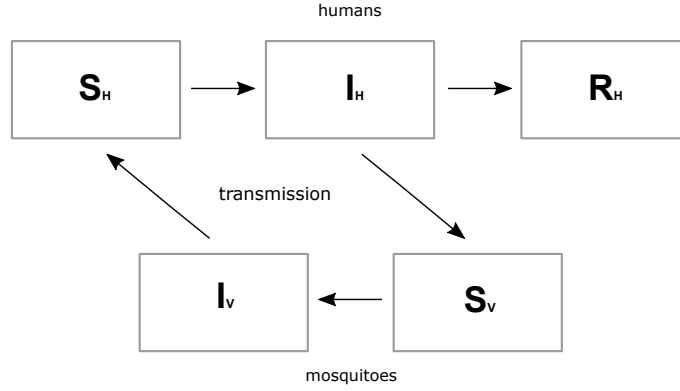


Figure 4: Structure of the SIR/SI model.

Mosquitoes are assumed to remain infectious for life. β_v is the transmission rate from humans to mosquitoes, β_H is the transmission rate from mosquitoes to humans, while $1/\gamma_H$ and $1/\mu_H$ are the mean infectious period and the mean lifespan of humans, $1/\mu_v$ is the mean lifespan of mosquitoes. N_H stands for the human population size and N_v is the mosquito population size. The mathematical model is written as follows:

$$\frac{dS_H}{dt}(t) = \mu_H N_H - \beta_H S_H(t) I_v(t) / N_v - \mu_H S_H(t), \quad (5)$$

$$\frac{dI_H}{dt}(t) = \beta_H S_H(t) I_v(t) / N_v - \gamma_H I_H(t) - \mu_H I_H(t), \quad (6)$$

$$\frac{dR_H}{dt}(t) = \gamma_H I_H(t) - \mu_H R_H(t) \quad (7)$$

$$\frac{dI_v}{dt}(t) = \beta_v S_v(t) I_H(t) / N_H - \mu_v I_v(t), \quad (8)$$

$$\frac{dS_v}{dt}(t) = -\beta_v S_v(t) I_H(t) / N_H + \mu_v I_v(t), \quad (9)$$

$$\frac{dC_i}{dt} = p\beta_H S_H(t) I_v(t) / N_v, \quad (10)$$

with the initial conditions in $t = t_0$

$$I_H(t_0) = I_{H0} > 0,$$

$$R_H(t_0) = R_{H0} > 0,$$

$$I_v(t_0) = I_{v0} > 0,$$

where I_{H0} , R_{H0} and I_{v0} are respectively, the initial number of infected people, the initial number of recovered people, and the initial number of infectious mosquitoes, respectively. As in the previous model, we use the cumulative number of infectives for identification purposes (equation 10).

Given the fact that the human population remains constant, one can express R_H in terms of the variables S_H and I_H , i.e. $R_H = N_H - S_H - I_H$, therefore equation 7 can be discarded and we can reduce the dimensionality of the system. A similar argument is true for the case of S_v in equation 9, i.e. $S_v = N_v - I_v$.

2.3. SEIR/SEI model

This model is based upon the work of Kucharski *et al.* (see [23]). This model incorporates a new compartment, exposed, for the human and the mosquito subpopulation which represents the number of individuals (and mosquitoes) that are incubating the virus, E_H (and E_v in the case of the vector population), i.e. where individuals (mosquitoes) are infected but are not able yet to transmit the virus. The inclusion of such a compartment into the model is due to the fact that it is known that vector and human populations incubate the virus for a number of days. Fig. 5 depicts the structure of this new model.

All parameters have the same connotation as in the SIR/SI model, and here $1/\kappa_H$ and $1/\kappa_v$ are the mean latent periods for humans and mosquitoes population respectively. The governing equations of the model follow:

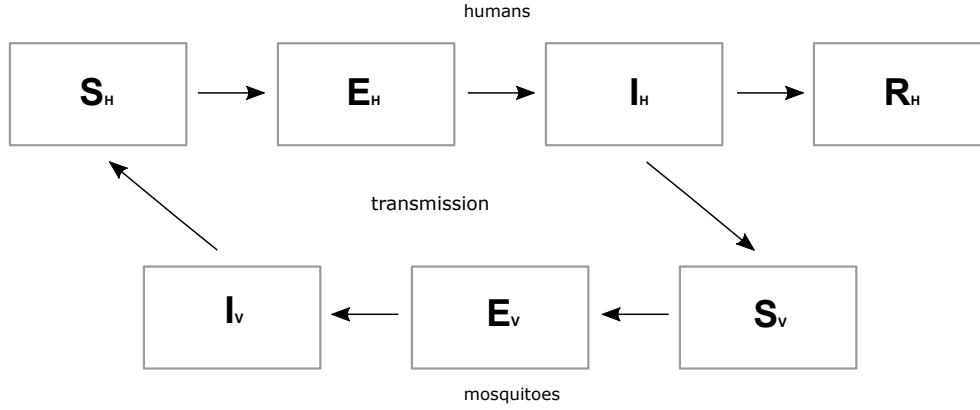


Figure 5: Structure of the SEIR/SEI model.

$$\frac{dS_H}{dt}(t) = \mu_H N_H - \beta_H S_H(t) I_v(t) / N_v - \mu_H S_H(t), \quad (11)$$

$$\frac{dE_H}{dt}(t) = \beta_H S_H(t) I_v(t) / N_v - \kappa_H E_H(t) - \mu_H E_H(t), \quad (12)$$

$$\frac{dI_H}{dt}(t) = \kappa_H E_H(t) - \gamma_H I_H(t) - \mu_H I_H(t), \quad (13)$$

$$R_H = N_H - S_H - I_H - E_H, \quad (14)$$

$$\frac{dE_v}{dt}(t) = \beta_v (S_v + E_v) I_H(t) / N_H - \kappa_v E_v(t) - \mu_v E_v(t), \quad (15)$$

$$\frac{dI_v}{dt}(t) = \kappa_v E_v(t) - \mu_v I_v(t), \quad (16)$$

$$S_v = N_v - I_v - E_v, \quad (17)$$

$$\frac{dC_i}{dt} = p \beta_H S_H(t) I_v(t) / N_v, \quad (18)$$

with the initial conditions in $t = t_0$

$$I_H(t_0) = I_{H0} > 0,$$

$$R_H(t_0) = R_{H0} > 0,$$

$$I_v(t_0) = I_{v0} > 0,$$

$$E_H(t_0) = E_{H0} > 0,$$

$$E_v(t_0) = E_{v0} > 0,$$

where I_{H0} , R_{H0} , I_{v0} , E_{H0} and E_{v0} are respectively, the initial number of infected people, the initial number of recovered people, the initial number of infectious mosquitoes, the initial number of people incubating the virus, and the initial number of mosquitoes incubating the virus, respectively. In equation 18, C_i accounts for the cumulative infectives and is a smooth monotone function that is used for identification purposes.

3. The basic reproductive ratio R_0

The basic reproductive ratio (see [10, 11] and [17]), R_0 , is defined as the expected number of secondary infections arising from a single individual during his or her entire infectious period, in a population of susceptibles. R_0 often serves as a threshold parameter that predicts whether an infection will spread. Determining R_0 is vital to understand and characterize the dynamics of the disease. However this crucial parameter is model dependent.

R_0 is the dominant eigenvalue of the so call “next generation matrix”. It is shown that, if $R_0 < 1$, then the disease free equilibrium is locally asymptotically stable; whereas if $R_0 > 1$, then it is unstable (see [32, 33]).

The basic reproduction number for the SIR model is known to be calculated as

$$R_0 = \frac{\beta}{\mu + \gamma}.$$

The basic reproduction number for the SIR/SI model is known to be calculated (see [27]) as:

$$R_0 = \frac{\beta_H \beta_v}{\mu_v (\mu_H + \gamma_H)}.$$

The basic reproduction number for the SEIR/SEI model is known to be calculated (the dominant eigenvalue of the next generation matrix, see [10, 11]) as:

$$R_0 = \frac{\beta_H \beta_v \kappa_v}{\mu_v \gamma_v (\kappa_v + \mu_v)}.$$

We study and calculate R_0 using different modelling perspectives that can allow us to draw better conclusions on its validity and range. Also, this pa-

parameter is investigated at different granularity levels: country wide and state wide.

4. Results

The used data used to validate the models, available on the internet, was published by Faria *et al.* [14, 13] while gathering information for their research. The data is partitioned by municipalities in Brazil, thus one may have different levels of granularity in the visualization of the data. By aggregation, of cases in different federal entities one can determine those entities that have the most reported cases. Table 1 shows the total number of cases throughout 2015 as reported in the epidemiological data provided.

In table 1 only those entities that report more than 100 cases in a year are displayed. One can see that the federal entity that reported the most number of cases is Bahía, followed by far by Alagoas, Ceará, and Rio Grande do Norte. All of these entities are located in the northeastern part of the country. The northeastern region is characterized by high temperatures (annual averages between 20 and 28 °C (68.0 and 82.4 °F), maxima of around 40 °C (104 °F)). During the months of June and July temperatures vary between 12 and 16 °C (53.6 and 60.8 °F) in the coastal regions, where most cases are reported.

Table 1: Reported cases in some entities of Brazil

Entities	Reported cases
Bahía (BA)	27290
Alagoas (AL)	497
Ceará (CE)	416
Rio Grande do Norte (RN)	264
Pará (PA)	155
Espírito Santo (ES)	125
Total Brazil	29639

The incidence data (left panels, images (a) to (d)) and the cumulative data used for identification purposes (right panels, images (e) to (h)) for the aggregated country data and most reported federal entities are shown in Fig. 6.

Relevant demographic information taken from the web page of the Instituto Brasileiro de Geografia e Estatística (IBGE) (2013) are given in table 2, where proportion refers to the proportion of reported cases to total population.

Table 2: Relevant demographic data

Parameter	Brazil	Bahía	Alagoas	Ceará
Population (MM)	207	15.15	8.86	3.32
Life expectancy (years)	75	71.9	69.2	72.4
Reported cases	29639	27290	416	497
Proportion	1.43e-4	1.80e-3	4.69e-5	1.491e-4

The life expectancy was used in all parameter estimations, thus reducing the number of free parameters to be identified.

A brief description on how to solve the system of ODEs associated to any of the three models proposed (SIR, SIR/SI and SEIR/SEI) is given in the appendix. The numerical models, which allow us to calculate the cumulative number of cases for each model, were implemented in language M of MATLAB. These functions will be used in the identification process of the unknown parameters, being 3, 6 and 10 the number of parameters for the SIR, SIR/SI and SEIR/SEI models respectively (see table 3).

It is important to note that the identification was performed over nondimensionalized systems.

The problem to be solved for the estimation of the unknown parameters is the following: Given a function $f(t)$ which represents the cumulative weekly number of cases for a period of 49 weeks during 2015, find the parameters x_i , $i = 1, \dots, n$ such that the answer $\tilde{f}(t)$ given by the model and the cumulative

incidence $f(t)$ are closed, that is

$$g(x_{min}) = \underset{x \in \Omega}{\text{global min}} g(x),$$

where $g : \Omega \subset \mathbb{R}^n \rightarrow \mathbb{R}$ defined by

$$g(t) = \int_0^T (f(t) - \tilde{f}(t))^2 dt$$

the mean squared error (MSE), $\Omega = \prod_{i=1}^n [a_i, b_i]$ and T is the time corresponding to the data.

It is important to point out that it is possible to find more than one set of parameters which satisfy the minimality condition required and related to the size of Ω . Also relevant is that every time the objective function needs to be evaluated, one run of the model has to be carried out.

The identification was carried through an exhaustive search procedure within the range of the different parameters involved in the model, not being the best available methodology because of the high number of evaluations of the objective function.

We considered feasible ranges for the parameters of the model whenever possible. Thus, according to epidemiological data, previously reported results [23, 31] and some sensibility carried out, the range considered for the parameters are in table 3.

We estimated the total of three unknown parameters for the SIR model (see table 4), six parameters for the SIR/SI model (see table 5), and ten parameters for the SEIR/SI model (see table 6), using the cumulative incidence suspicious data. Cumulative incidence is generally smoother than the original incidence data and thus easier to fit.

The numerical solutions of the models were performed using Matlab and compared to the cumulative data to obtain a mean squared error (MSE). Those parameters that produced the smallest errors are reported as the best identification for the data. In all cases the basic reproduction number is reported as well as the MSE.

Table 3: Ranges for the estimation of the models unknown parameters.

Model Parameter	SIR	SIR/SI	SEIR/SEI	reference for the reciprocal
β_H (day^{-1})	[0.01,0.6]	[0.01,0.6]	[0.1,1.2]	-
γ_H (day^{-1})	[0.1,0.4]	[0.1,0.5]	[0.1,0.5]	2-9 days
β_v (day^{-1})	-	[0.01,0.4]	[0.01,0.3]	-
μ_v (day^{-1})	-	[0.03,0.3]	[0.03,0.3]	4-30 days
κ_H (day^{-1})	-	-	[0.083,0.34]	3-12 days
κ_v (day^{-1})	-	-	[0.20,0.50]	2-5 days
I_{v0}	-	[1.e-9,5.e-5]	[8.e-7,5.e-5]	-
E_0	-	-	[8.e-7,9.e-6]	-
E_{v0}	-	-	[8.e-7,9.e-6]	-
p	[1.e-5,6.e-3]	[1.e-5,6.e-3]	[4.e-5,6.e-3]	-

Table 4: Estimated parameters for the SIR model.

Parameter	Brazil	Bahía	Alagoas	Ceará
β_H	0.4340	0.1954	0.26767	0.46124
γ_H	0.3816	0.1493	0.21576	0.40667
p	5.7931e-4	4.0204e-3	4.0912e-4	2.0506e-4
R_0	1.137	1.274	1.2382	1.1336
Error	2.2406e-3	9.4618e-4	4.1092e-3	2.4544e-3

Table 5: Estimated parameters for the SIR/SI model.

Parameter	Brazil	Bahía	Alagoas	Ceará
β_H	0.49368	0.48947	0.31889	0.54211
γ_H	0.21263	0.11	0.36333	0.31053
β_v	0.038947	0.037474	0.36000	0.15474
μ_v	0.0333	0.05	0.22	0.15667
I_{v0}	3.4526e-5	1e-7	3e-8	1e-9
p	1.5263e-4	1.6632e-3	2.7778e-4	6.8737e-5
R_0	2.715	3.3338	1.436	1.724
Error	7.0798e-4	6.0564e-3	2.9883e-3	7.6298e-4

Fig. 6 overlays the cumulative reported data points with the simulated cumulative cases with the best set of parameters for each entity (right panels) and the 3 models investigated. Although incidence data was not used in the identification purposes, left panel on the left show an overlay of the incidence data with the simulated incidence.

5. Discussion

In this work we identified three models for the Zika virus in Brasil. The models were identified using the aggregated data for the country and then for 3 federal entities, namely Bahia, Alagoas and Ceará, which were the areas with the greatest number of cases reported. One aspect worth mentioning is that the majority of the cases came from Bahía. One can see from the results in tables 5, and 6 that the model parameters are similar for the aggregated data (Brazil) and the federal region with most numbered cases. This is so for those models that include the vector within the models, namely the SIR/SI and SEIR/SEI. However, this is not maintained in the more basic SIR model (see Table 4).

For the SIR model, the results for Ceará and the aggregated Brazil cases are similar according to the estimated parameters, while Bahía and Alagoas seemed

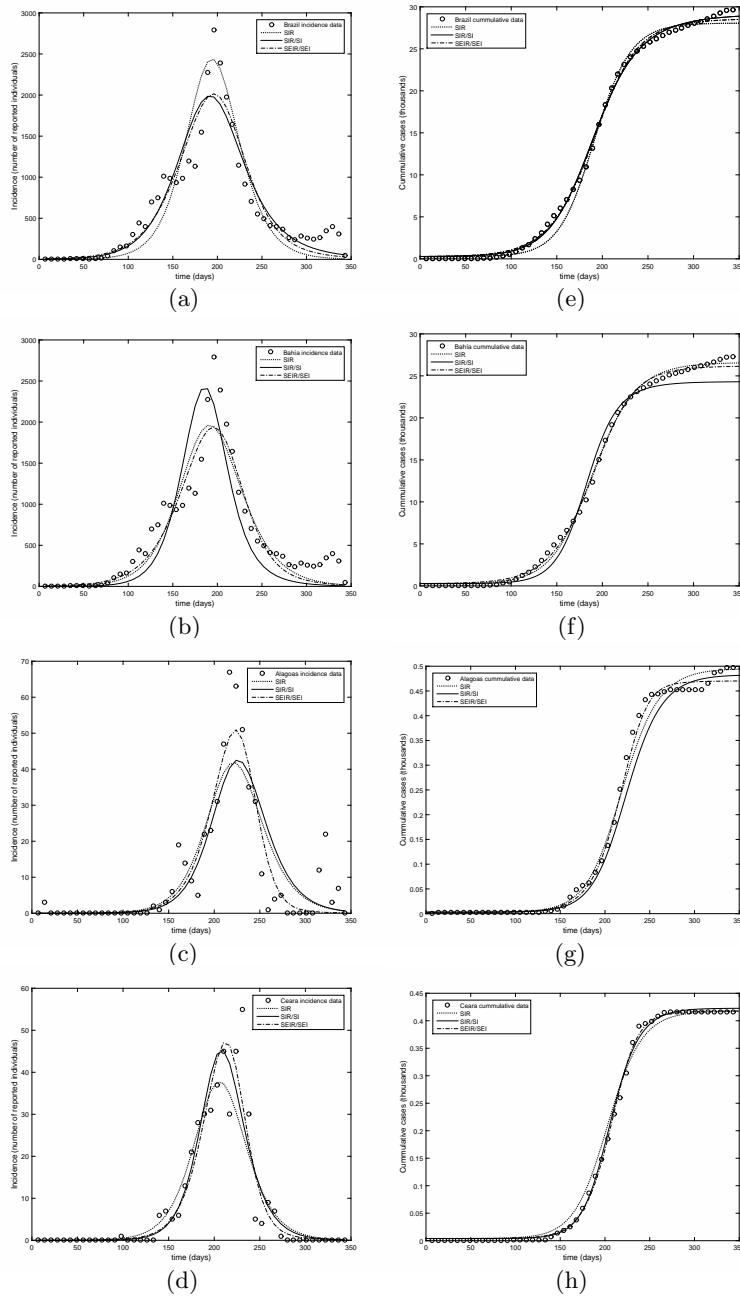


Figure 6: Incidence (images (a) to (d)) and cumulative (images (e) to (h)) data and model results for Brazil ((a) and (e)), Bahía ((b) and (f)), Alagoas ((c) and (g)) and Ceará ((d) and (h)). Points marked with circles in (a) to (d) correspond to incidence data and in (e) to (h) correspond to cumulative data. Dashed, solid, and dashdotted lines represent SIR, SIR/SI and SEIR/SEI models respectively.

Table 6: Estimated parameters for the SEIR/SEI model.

Parameter	Brazil	Bahía	Alagoas	Ceará
β_H	0.86372	0.84	0.8	1.1
γ_H	0.28333	0.19667	0.11	0.305
β_v	0.045	0.04	0.040556	0.06
μ_v	0.03333	0.03333	0.03333	0.03333
κ_H	0.083	0.083	0.083	0.083
κ_v	0.425	0.2	0.2	0.5
I_{v0}	5.e-5	5.e-5	8.e-7	1.e-8
E_0	9.e-6	9.e-6	8.e-7	6.e-7
E_{v0}	4.9e-6	6.95e-6	8e-7	6.e-7
p	0.00014	0.00173	0.00014	0.000046667
R_0	3.8165	4.3936	7.5854	6.0867
Error	0.00081171	0.00089141	0.0015467	0.00052088

tuned into one another. This result is in agreement with the proportions calculated in Table 2 for Brazil and Ceará, but they do not agree when comparing Bahía and Alagoas since there is a difference in two orders of magnitude. But the models adjust best to similar contact and infectious rates. It is noteworthy however that the R_0 is within similar ranges (1.1 - 1.3), see [27] with $R_0 = 1.10$ for SIR model, but far from the ranges reported in other Zika outbreaks, see [26] ($R_0 = 4.3 - 5.8$ for the Yap Island epidemic and $R_0 = 1.8 - 2.2$ for the French Polynesia epidemic), and [34] ($R_0 = 1.57$ for the SIR model, $R_0 = 1.65$ using a SEIR model, and $R_0 = 1.66$ for a more complicated model, all applied to influenza A). One reason could be that the R_0 is model dependent and in this case this very simple model does not include important infectious factor such as the vector population. Therefore, we regard this model to be non-informative and too simplistic for the situation being modelled, and it was considered for comparison purposes and as a parsimonious model. When the vector population

is included the ranges of the values for R_0 expand and the values are bigger. For the SIR/SI model the range is (1.4 - 3.3) and for the SEIR/SEI model the range is (3.8 - 7.5), this could be due to model dependency of R_0 . Although the ranges for the R_0 are disjunct, these are consistent with other reported values in the literature, see [31] with $R_0 = 4.4$ with 95% CI [3.0, 6.2] and a one standard deviation uncertainty of 0.9 for the outbreak of ZIKV that began in 2015 in Barranquilla, Colombia using the SEIR/SEI model, [27] with $R_0 = 1.57$ using a vector-host model, and [23] with R_0 ranged for from 2.6 (95Marquises to 4.8 (95% CI: 3.28.4) in Moorea for French Polynesia ZIKV outbreak using the SEIR/SEI model.

Even though the models that included the vector population have more free parameters to adjust and identify, allowing for greater degrees of freedom, the errors in the adjustments are similar for all three models used. Furthermore, all three models follow the data very well as one can see on the (e) to (h) panels in Fig. 6. Even though the incidence data was not used during the identification process, panels (a) to (d) from Figure Fig. 6 overlays the data with the induced incidence curve with the model parameters found. In the case of Brazil, the SIR model was able to best capture the rise in the incidence around the peak of infectiousness (day 200), but for the subregions the models that incorporated the vector population best captured such rise.

One point to mention is that the Brazil data aggregates information from varying regions with varying forms and times of outbreak, which makes the interpretation of the results difficult.

Acknowledgements

This research did not receive any specific grant from funding agencies in the public, commercial, or not-for-profit sectors.

References

References

- [1] B. Berkowitz, L. Karklis, S. Tan, D. Lu, P. Clark, What you need to know about the zika virus, The Washington Post, <https://www.washingtonpost.com/graphics/health/zika-virus/> (2016).
- [2] A. Bernardo, Sospechan que el zika podría afectar al cerebro de adultos, Hipertextual, <https://hipertextual.com/2016/08/zika-cerebro-adultos> (8 2016).
- [3] P. Brasil, J. Pereira, C. Raja Gabaglia, L. Damasceno, M. Wakimoto, R. Ribeiro Nogueira, P. Carvalho de Sequeira, A. Machado Siqueira, L. Abreu de Carvalho, D. Cotrim da Cunha, G. Calvet, E. Neves, M. Moreira, A. Rodrigues-Bai/ ao, P. Nassar de Carvalho, C. Janzen, S. Valderamos, J. Cherry, A. Bispo de Filippis, K. Nielsen Saines, Zika virus infection in pregnant women in rio de janeiro - preliminary report, The New England Journal of Medicine, doi: 10.1056/NEJMoa1602412 (3 2016).
- [4] F. Brauer, C. Castillo-Chavez, Mathematical Models in Population Biology and Epidemiology, 2nd ed., Springer, 2012, ISBN 978-1-4614-1685-2.
- [5] F. Brauer, C. Castillo-Chavez, E. De La Pava-Salgado, K. Barley, C. Castillo-Garsow, D. Chowell, B. Espinoza, P. Gonzalez Parra, C. Hernandez Surez, V. Moreno, Modelos de la propagación de enfermedades infecciosas, Universidad Autnoma de Occidente, Cali, Colombia, 2015, ISBN 978-958-8713-65-6.
- [6] J. Brownlee, Certain considerations regarding the epidemiology of phthisis pulmonalis, Public Health 29 (1916) 130–145, doi: 10.1016/S0033-3506(15)80528-9.
- [7] S. Buitrago, R. Escalante, M. Villazana, Modelización matemática da la expansión del virus zika en la región Latinamericana, in: Simulación y

Aplicaciones Recientes para Ciencia y Tecnología, Ed: Y. Gnzales, E. Dvila, V. Duarte, M.V. Candal, O. Pelliccioni, J. Darias, M. Cerrolaza, 2016, ISBN 978-980-7161-05-3.

- [8] G. Calvet, R. Aguiar, A. Melo, S. Sampaio, I. de Filippis, A. Fabri, E. Araujo, P. de Sequeira, M. de Mendona, L. de Oliveira, D. Tschoeke, C. Schrago, F. Thompson, P. Brasil, F. dos Santos, R. Nogueira, A. Tanuri, A. de Filippis, Detection and sequencing of zika virus from amniotic fluid of fetuses with microcephaly in brazil: a case study, *The Lancet Infectious Diseases* 16 (6) (2016) 653–660, doi: 10.1016/S1473-3099(16)00095-5.
- [9] G. Dick, S. Kitchen, A. Haddow, Zika virus (i). isolations and serological specificity, *Trans. R. Soc. Trop. Med. Hyg.* 46 (1952) 509–520, doi: 10.1016/0035-9203(52)90042-4.
- [10] O. Diekmann, J. Heesterbeek, J. Matz, On the definition and computation of the basic reproduction ratio R_0 in models for infectious diseases in heterogeneous populations, *Journal of Mathematical Biology* 28 (4) (1990) 365–382, doi: 10.1007/BF00178324.
- [11] O. Diekmann, J. Heesterbeek, M. Roberts, The construction of next-generation matrices for compartmental epidemic models, *Journal of the Royal Society Interface* 7 (47) (2010) 873–885, doi: 10.1098/rsif.2009.0386.
- [12] V. Farewell, T. Johnson, Commentary: Dr john brownlee ma, md, dsc, dph (cantab), frfps, fss, frmets (18681927), public health officer, geneticist, epidemiologist and medical statistician, *International Journal of Epidemiology* 42 (2013) 935–943, doi: 10.1093/ije/dyt067.
- [13] N. Faria, R. Azevedo, M. Kraemer, et al., Data from: Zika virus in the americas: early epidemiological and genetic findings, *Dryad Digital Repository*, doi: 10.5061/dryad.6kn23 (2016).
- [14] N. Faria, R. Azevedo, M. Kraemer, et al., Zika virus in the americas: early

- epidemiological and genetic findings, *Science* 352 (6283) (2016) 345–349, doi: 10.1126/science.aaf5036.
- [15] O. Faye, O. Faye, D. Diallo, M. Diallo, M. Weidmann, A. Sall, Quantitative real-time pcr detection of zika virus and evaluation with field-caught mosquitoes, *Viol. J.* 10 (311) (2013) 1–8, doi: 10.1186/1743-422X-10-311.
- [16] V. Greenwood, New insights into how zika harms the brain, *Quanta Magazine*, <https://www.quantamagazine.org/20160707-how-zika-interferes-with-brain-development/> (2016).
- [17] J. Heffernan, R. Smith, L. Wahl, Perspectives on the basic reproductive ratio, *Journal of The Royal Society Interface*, doi: 10.1098/rsif.2005.0042 (2005).
- [18] S. Ios, H. Mallet, I. Leparç-Goffart, V. Gauthier, T. Cardoso, M. Herida, Current zika virus epidemiology and recent epidemics, *Med. Mal. Infect.* 44 (7) (2014) 302–307, doi: 10.1016/j.medmal.2014.04.008.
- [19] M. Johansson, L. Mier y Teran Romero, J. Reefhuis, S. Gilboa, S. Hills, Zika and the risk of microcephaly, *New England Journal of Medicine* 375 (2016) 1–4, doi: 10.1056/NEJMp1605367.
- [20] W. Kermack, A. McKendrick, A contribution to the mathematical theory of epidemics, *Proc. Royal Soc. London* 115 (1927) 700–721, doi: 10.1098/rspa.1927.0118.
- [21] W. Kermack, A. McKendrick, A contribution to the mathematical theory of epidemics, part ii, *Proc. Royal Soc. London* 138 (1932) 55–83, <http://www.math.utah.edu/~bkohler/Journalclub/kermack1932.pdf>.
- [22] W. Kermack, A. McKendrick, A contribution to the mathematical theory of epidemics, part iii, *Proc. Royal Soc. London* 141 (1933) 94–112, <http://www.uvm.edu/pdodds/files/papers/others/1933/kermack1933.pdf>.

- [23] A. Kucharski, S. Funk, R. Eggo, H. Mallet, W. Edmunds, E. Nilles, Transmission dynamics of zika virus in island populations: A modelling analysis of the 2013-14 french polynesia outbreak, *PLoS Negl Trop Dis* 10 (5) (2016) 1–15, doi: 10.1371/journal.pntd.0004726.
- [24] C. Li, D. Xu, Q. Ye, S. Hong, Y. Jiang, X. Liu, N. Zhang, L. Shi, C.-F. Qin, Z. Xu, Zika virus disrupts neural progenitor development and leads to microcephaly in mice, *Cell Stem Cell* 19 (1) (2016) 120–126, doi: 10.1016/j.stem.2016.04.017.
- [25] H. Li, L. Saucedo Cuevas, J. Regla Nava, A. Terskikh, S. Shresta, J. Gleeson, Zika virus infects neural progenitors in the adult mouse brain and alters proliferation, *Cell Stem Cell* 19 (2016) 1–6, doi: 10.1016/j.stem.2016.08.005.
- [26] H. Nishiura, R. Kinoshita, K. Mizumoto, Y. Y., K. Nah, Transmission potential of zika virus infection in the south pacific, *International Journal of Infectious Diseases* 45 (2016) 95–97, doi: 10.1016/j.ijid.2016.02.017.
- [27] A. Pandey, A. Mubayi, J. Medlock, Comparing vector-host and sir models for dengue transmission, *Mathematical Biosciences* 246 (2) (2013) 252–259, doi: 10.1016/j.mbs.2013.10.007.
- [28] H. Retallack, E. Di-Lullo, C. Arias, K. Knopp, C. Sandoval Espinosa, M. Laurie, Y. Zhou, M. Gormley, W. Mancía Leon, R. Krencik, E. Ullian, J. Spatazza, A. Pollen, K. Ona, T. Nowakowski, J. DeRisi, S. Fisher, A. Kriegstein, Zika virus in the human placenta and developing brain: Cell tropism and drug inhibition, *bioRxiv*, The preprint server for biology, doi: 10.1101/058883 (2016).
- [29] R. Ross, *The Prevention of Malaria*, 2nd ed., John Murray, London, 1911.
- [30] H. Tang, C. Hammack, S. Ogden, Z. Wen, X. Qian, Y. Li, B. Yao, J. Shin, F. Zhang, E. Lee, K. Christian, R. Didier, P. Jin, H. Song, G. Ming, Zika

virus infects human cortical neural progenitors and attenuates their growth, *Cell Stem Cell* 18 (2016) 587–590, doi: 10.1016/j.stem.2016.02.016.

- [31] S. Towers, F. Brauer, C. Castillo-Chavez, A. Falconar, A. Mubayi, C. Romero-Vivas, Estimation of the reproduction number of the 2015 zika virus outbreak in barranquilla, colombia, and a first estimate of the relative role of sexual transmission, ResearchGate, <https://www.researchgate.net/publication/303821853> (2016).
- [32] P. van den Driessche, W. J., Reproduction numbers and sub-threshold endemic equilibria for compartmental models of disease transmission, *Mathematical Biosciences* 180 (1-2) (2002) 29–48, doi: 10.1016/S0025-5564(02)00108-6.
- [33] P. van den Driessche, W. J., Further notes on the basic reproduction number, in: *Mathematical Epidemiology*, vol. 1945 of Lecture Notes in Mathematics, chap. 6, Springer, Berlin Heidelberg, 2008, pp. 159–178, doi: 10.1007/978-3-540-78911-6_6.
- [34] J. Wallinga, M. Lipsitch, How generation intervals shape the relationship between growth rates and reproductive numbers, *Proceeding of the Royal Society B* 274 (2007) 599–604, doi: 10.1098/rspb.2006.3754.
- [35] WHO, Zika strategic response plan, revised for july 2016 december 2017, Tech. rep., World Health Organization, <http://reliefweb.int/sites/reliefweb.int/files/resources/WHO-ZIKV-SRF-16.3-eng.pdf> (june 2016).

Appendix - Discretizing the models

In order to exemplify the discretization methodology, the SIR/SI model (equations 5 to 10) will be used. Given the fact that the human population remains constant, one can express R_H in terms of the variables S_H and I_H , i.e. $R_H = N_H - S_H - I_H$, therefore, equation 7 for this model can be discarded and

we can reduce the dimensionality of the system. A similar argument is true for the case of S_v in equation 9, i.e. $S_v = N_v - I_v$. Finally, the following system of ordinary differential equations with initial conditions has to be solved.

$$\frac{dS_H}{dt}(t) = \mu_H N_H - \beta_H S_H(t) I_v(t) / N_v - \mu_H S_H(t), \quad (19)$$

$$\frac{dI_H}{dt}(t) = \beta_H S_H(t) I_v(t) / N_v - \gamma_H I_H(t) - \mu_H I_H(t), \quad (20)$$

$$R_H = N_H - S_H - I_H \quad (21)$$

$$\frac{dI_v}{dt}(t) = \beta_v S_v(t) I_H(t) / N_H - \mu_v I_v(t), \quad (22)$$

$$S_v = N_v - I_v, \quad (23)$$

$$\frac{dC}{dt} = p\beta_H S_H(t) I_v(t) / N_v, \quad (24)$$

with the initial conditions in $t = t_0$

$$I_H(t_0) = I_{H0} > 0,$$

$$R_H(t_0) = R_{H0} > 0,$$

$$I_v(t_0) = I_{v0} > 0.$$

The following step is the normalization of this system, i.e. with

$$s_H = S_H / N_H, \quad i_h = I_H / N_H, \quad r_H = R_H / N_H,$$

$$i_v = I_v / N_v, \quad s_v = S_v / N_v, \quad c = C / N_H,$$

the following equivalent system of ODEs arises

$$\frac{ds_H}{dt}(t) = \mu_H - \beta_H s_H(t) i_v(t) - \mu_H s_H(t), \quad (25)$$

$$\frac{di_H}{dt}(t) = \beta_H s_H(t) i_v(t) - \gamma_H i_H(t) - \mu_H i_H(t), \quad (26)$$

$$r_H = 1 - s_H - i_H \quad (27)$$

$$\frac{di_v}{dt}(t) = \beta_v s_v(t) i_H(t) - \mu_v i_v(t), \quad (28)$$

$$s_v = 1 - i_v, \quad (29)$$

$$\frac{dc}{dt} = p\beta_H s_H(t) i_v(t). \quad (30)$$

The basic idea of any approximation method is to replace the original problem by another problem that is easier to solve and whose solution is, in some sense, close to the solution of the original problem.

Given $M \in \mathbb{N}$, let $\{t_i\}_{1 \leq i \leq M}$ be an uniform subdivision of the time domain, with mesh length $h = \Delta t = t_{i+1} - t_i$ along the direction t .

The following is the forward finite difference for the first order operator

$$\left(\frac{df}{dt}\right)_{i+1} = \frac{f(t_i + h) - f(t_i)}{h} \text{ for } 1 \leq i \leq M - 1$$

where f represents the functions s_H, i_H, r_H, i_v, s_v and c .

Finally the following set of linear equations arises upon substitution of the forward finite difference operator

$$s_H(t_i + h) = s_H(t_i) + \mu_H h - \beta_H s_H(t_i) i_v(t_i) h - \mu_H s_H(t_i) h, \quad (31)$$

$$i_H(t_i + h) = i_H(t_i) + \beta_H s_H(t_i) i_v(t_i) h - \gamma_H i_H(t_i) h - \mu_H i_H(t_i) h, \quad (32)$$

$$r_H(t_i + h) = 1 - s_H(t_i + h) - i_H(t_i + h) \quad (33)$$

$$i_v(t_i + h) = i_v(t_i) + \beta_v s_v(t_i) i_H(t_i) h - \mu_v i_v(t_i) h, \quad (34)$$

$$s_v(t_i + h) = 1 - i_v(t_i + h), \quad (35)$$

$$c(t_i + h) = c(t_i) + p \beta_H s_H(t_i) i_v(t_i) h, \quad (36)$$

for $1 \leq i \leq M - 1$.

The numerical model (equations 31 to 36) was implemented using the M languages of MATLAB.